

Direct Numerical Simulations of Fundamental Turbulent Flows with the World's Largest Number of Grid-points and Application to Modeling of Engineering Turbulent Flows

Project Representative

Yukio Kaneda Graduate School of Engineering, Nagoya University

Authors

Yukio Kaneda Graduate School of Engineering, Nagoya University

Takashi Ishihara Graduate School of Engineering, Nagoya University

Kaoru Iwamoto Mechanical Systems Engineering, Tokyo University of Agriculture and Technology

Tetsuro Tamura Interdisciplinary Graduate School of Science and Engineering, Tokyo Institute of Technology

Yasuo Kawaguchi Department of Mechanical Engineering, Tokyo University of Science

Takahiro Tsukahara Department of Mechanical Engineering, Tokyo University of Science

We performed high-resolution direct numerical simulations (DNSs) of canonical turbulent flows on the Earth Simulator 2. They include (i) turbulent channel flow, (ii) quasi-static MHD turbulence in an imposed magnetic field, and (iii) turbulent boundary layer on sinusoidal wavy walls. The DNSs provide invaluable data for the following studies, respectively; (1) the local anisotropy in small-scale statistics in the log-law layer of turbulent channel flow, (2) anisotropy and intermittency of quasi-static MHD turbulence in an imposed magnetic field, and (3) the effect of the wave length of the sinusoidal wavy wall upon the turbulent statistics. By the analysis of the DNS data, it was shown that (1) the local anisotropy decreases with the distance from the boundary wall, (2) the magnetic field enhances the intermittency, and (3) the pressure drag decreases with the wavelength of the sinusoidal wavy wall. We also performed the following turbulence simulations for environmental and industrial applications; (i) Large Eddy Simulation of turbulent boundary layer over homogenous vegetation field using a hybrid LES-RANS model which can represent appropriately and efficiently the roughness condition on ground surface, and (ii) DNS of turbulent flows of non-Newtonian surfactant solution in a channel with rectangular orifices. By (ii), we could estimate the characteristics of the heat transfer associated with the drag reduction.

Keywords: High-resolution DNS, turbulent channel flow, MHD turbulence, turbulent boundary layer, rough wall, LES, urban turbulent boundary layer, non-Newtonian fluid, drag reduction

1. Direct numerical simulations of fundamental turbulent flows

1.1 High resolution DNS of turbulent channel flow

In order to study the small-scale statistics of high-Reynolds number wall-bounded turbulence, we performed a direct numerical simulation (DNS) of turbulent channel flow (TCF) of an incompressible fluid obeying the Navier-Stokes (NS) equations, in a computational box with streamwise (x) and spanwise (z) periodicities ($L_x = 2\pi h$ and $L_z = \pi h$), at a Reynolds number $Re_\tau = 2560$ based on the friction velocity u_τ and the channel half-width h . We achieved the sustained performance of 6.1Tflops (11.7% of the peak performance) in the DNS of TCF on 2048x1536x2048 grid points using 64 nodes of ES2. The numbers of grid points as well as the computational domain size in the x and z directions are twice as large as our previous DNS.

The DNS is based on the Fourier-spectral method in x - and z -directions, and the Chebyshev-tau method in the wall-normal y -direction. The alias errors are removed by the 3/2 rule. The NS equations are expressed in terms of the wall-normal vorticity components and the Laplacian of wall-normal velocity. Time advancement is accomplished by a third-order Runge-Kutta method for the convection term and the first-order implicit Euler method for the viscous terms. Our DNS has been advanced up to $t = 2.2 t_w$, where t_w is the wash-out time. We have to perform the DNS until $t > 10t_w$ to obtain more reliable statistics, and to elucidate the finite box size effect on the possible universality in the small-scale statistics.

Figure 1 shows the comparison between compensated longitudinal spectra $E_{11}(k_x)$ and $E_{33}(k_z)$ obtained in our previous DNS in the smaller domain; E_{11} is for the streamwise (x)

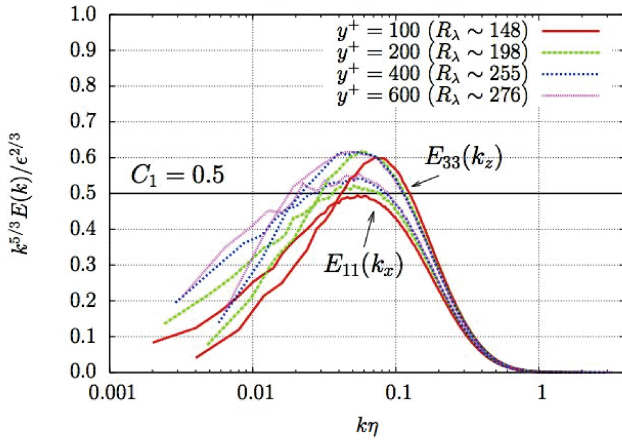


Fig. 1 Comparison between compensated longitudinal spectra $E_{11}(k_x)$ and $E_{33}(k_z)$, at $y^+ = 100, 200, 400$ and 600 in the TCF obtained by the DNS with $1024 \times 1536 \times 1024$ grid points and $Re_\tau = 2560$. η is Kolmogorov's length scale. Solid line is the K41 spectrum $k^{5/3}E(k)/\epsilon^{2/3} = C_1$ with $C_1 = 0.5$.

velocity component and E_{33} is for the span-wise (z) component. The classical value for the Kolmogorov constant $C_1 = 0.5$ is also shown in Fig.1. It is shown that there is a wavenumber range in which each spectrum is not far from the K41 spectra. The difference between $E_{11}(k_x)$ and $E_{33}(k_z)$ is seen in Fig. 1 to decrease with the increase of the Taylor scale Reynolds number Re_λ (Note that Re_λ is a function of the distance from the wall).

1.2 DNS of quasi-static magnetohydrodynamic (MHD) turbulence

Low-magnetic-Reynolds-number magnetohydrodynamic (MHD) turbulence in an imposed magnetic field widely exists in industrial applications, such as electro-magnetic processing

of materials in metallurgical industry. When the magnetic Reynolds number is sufficiently small, we can apply the so-called quasi-static approximation to the MHD turbulence.

Quasi-static MHD turbulence is characterized by multiscale anisotropy and intermittency. Wavelet representation is an efficient way to analyze such intermittent data, since wavelets are well localized in space, scale and direction. To quantify intermittency in anisotropic turbulence, Bos *et al.* [1] introduced scale- and direction-dependent statistics using three-dimensional orthonormal discrete wavelets.

In this study, we performed high-resolution DNSs of incompressible quasi-static MHD turbulence at the two interaction parameters, i.e. $N=1$ and 3 , with 512^3 grid points on the ES and examined the anisotropy and intermittency of the obtained DNS fields, using the scale- and direction-dependent statistics [1].

We found that for the $N=3$, the imposed magnetic field plays a major role on the increase of intermittency in the direction parallel to the magnetic field. The details of the current study are shown in [2].

2. DNS of turbulent boundary layer on rough walls

Turbulent boundary layer on rough plates is one of the most important problems in fundamental turbulent heat transfer research, practical engineering applications and environmental processes. DNS of turbulent boundary layer on rough walls has been barely performed compared with that of other wall-bounded turbulence such as turbulent channel flows.

In this study, direct numerical simulation of turbulent boundary layer with several sinusoidal wavy walls has been performed in order to investigate the effect of the wave length

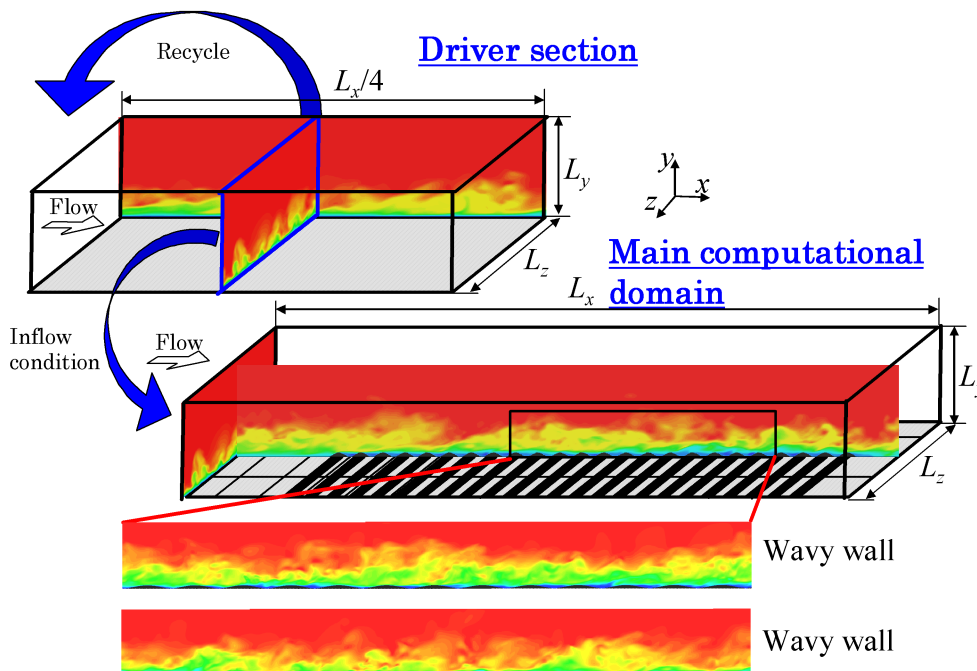


Fig. 2 Computational domains for turbulent boundary layer on several sinusoidal wavy walls.

of the sinusoidal wavy wall, λ , upon the turbulent statistics. The amplitude of the sinusoidal wavy wall, a , was kept constant in wall units, and the wave length was set to be $a / \lambda = 0.011, 0.022$ and 0.033 . For the spatially developing boundary layers on sinusoidal wavy walls, we provided a driver section with a flat wall and an analysis section with a sinusoidal wavy wall as shown in Fig. 2. Turbulent inflow conditions for the driver section are generated by rescaling the turbulent boundary layer at some distance downstream of the inflow and by reintroducing the recycled mean profile and fluctuation field. This technique follows those of Kong et al. [3] and Lund et al. [4]. Turbulent inflow conditions for the analysis section, on the other hand, are generated by exactly copying a turbulent field of the driver section. The parallel and vectorization efficiencies are 98.43% and 99.50%, respectively.

The average of the wall shear stress hardly changes with decreasing the wave length, whilst the friction coefficient, which was defined as the summation of the wall shear stress and the pressure drag, was increased with decreasing the wave length owing to the increase of the pressure drag (not shown here).

3. Application of LES of turbulent flows to urban environmental and strong wind disaster problems

Based on the fundamental knowledge of turbulent flows, we extend the LES techniques to atmospheric phenomena appearing as an environmental as well as a strong wind disaster problem which are strongly related with the human society.

Firstly, Large Eddy Simulation (LES) of a turbulent boundary flow over homogenous vegetation field was performed using hybrid LES-RANS model which can represent appropriately and efficiently the roughness condition on ground surface [5]. In LES of boundary layer flows over vegetation fields, leaves and plants are too thin to resolve them by the sufficient number of grid points. So, the effect of those leaves and plants on the flow must be treated with an artificial model. The turbulence closure model for plant canopy flows used here was proposed by Hiraoka and Ohashi [6], which is formulated based on RANS ($k-\epsilon$) turbulence model. The computational domain is 2.5 km long x 0.4 km wide and its horizontal resolution is 5 m long x 2.5 m wide. The quasi-periodic boundary condition is employed in streamwise direction (Fig. 3). The boundary layer thickness reaches to approximately 500 m and the mean velocity profile

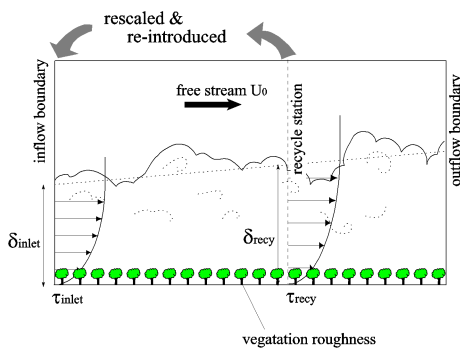


Fig. 3 Computational region and concept of the quasi-periodic boundary condition for a turbulent boundary layer flow over vegetation field.

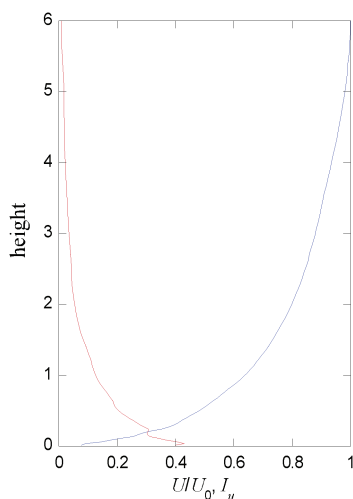
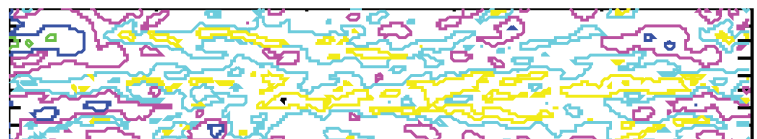
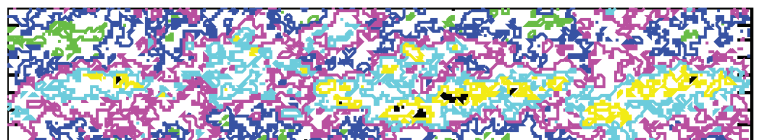


Fig. 4 Mean velocity and turbulence intensity profiles.



(a) RANS region



(b) LES region

Fig. 5 Contour of streamwise velocity.

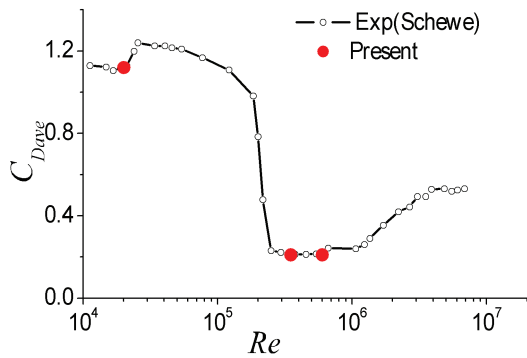


Fig. 6 Drastic change in drag coefficient at the very high Reynolds numbers.

and turbulence intensity reasonably fit to those obtained by the previous experimental study (Fig. 4). It can be seen that the turbulence structure in LES region is very small and fine compared to that in RANS region (Fig. 5).

Recent architectural buildings have a variety of shapes based on unique designer concepts, and the curved surfaces are frequently used for building wall. Here, as a typical and a fundamental case in such buildings, a circular cylinder is focused on. The flow characteristics around a circular cylinder in realistic high Reynolds number region are investigated by use of the LES model. As a result, the present LES model succeeded in accurately simulating the drastic change of aerodynamic coefficient (Fig. 6). Also, details of the flow structures near separating and reattaching region are clarified by visualization of the computed data (Fig. 7).

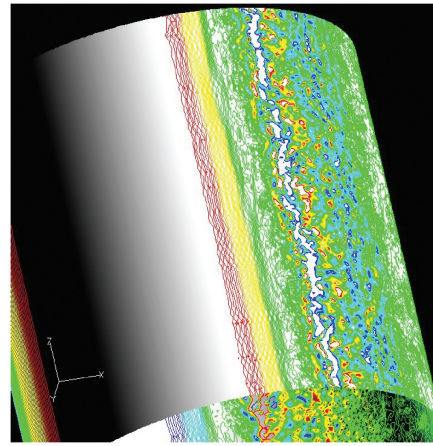


Fig. 7 Three-dimensional flow structures near separating and reattaching region.

4. DNS of the turbulence in non-Newtonian surfactant solution

The effect of polymer or surfactant additives on turbulent flow has received much attention from both practical and scientific perspectives since the discovery in the 1940s, that is, small additive concentration can lead to significant reduction in drag of 50% or greater [7]. This phenomenon is of practical importance and has recently been implemented in several industrial systems to save energy. In general, the solution used as a working fluid for such a drag-reducing flow is a viscoelastic (non-Newtonian) liquid. The properties of the liquid solution measured even in simple shear or extensional flows are known to exhibit appreciably different from those of the pure solvent. The goal of the present work is to better understand the physics of viscoelastic turbulent flow, particularly in the context of complicated flow geometry.

Many DNS of polymer-induced drag reduction were performed for various types of canonical flows, such as

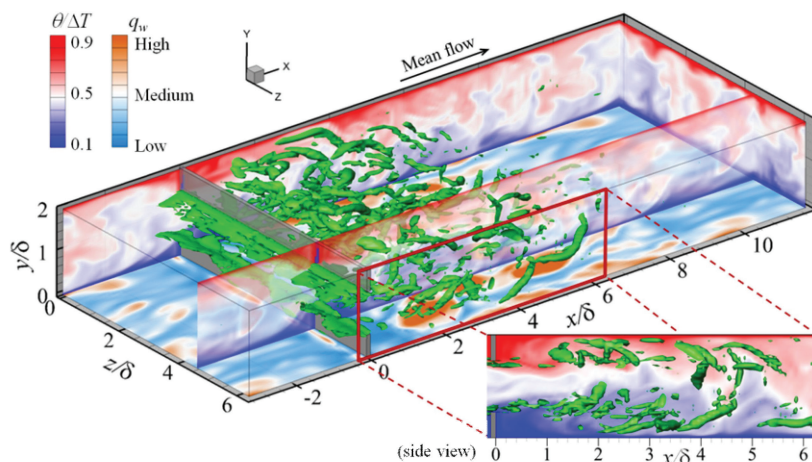


Fig. 8 Instantaneous flow and thermal field in viscoelastic turbulent flow through a rectangular rib (at $x = 0$ with 0.1δ thickness): green isosurface, vortex identified by the second invariant of strain tensor; contours, temperature or wall heat flux. Thermal boundary condition is the constant temperature difference between two walls ($y = 0$ and 2δ), the periodic condition is applied in x and z .

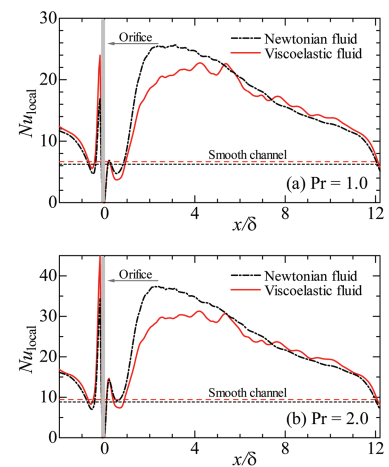


Fig. 9 Local Nusselt-number profile as a function of x , for different Prandtl numbers. Also shown are estimated values in the case of a smooth channel at the same bulk Reynolds number.

isotropic turbulence, shear-driven turbulence, channel flow, and boundary layer. Although flows through complicated geometries have been studied by a number of researchers for the laminar regime for both Newtonian and viscoelastic fluids [8], those under turbulent conditions have received much less attention, except that Makino *et al.* [9] carried out DNS of the turbulent 'Newtonian' flow in a channel with periodic rectangular orifices. Further, it should be noted that, to the authors' knowledge, there has never been any DNS of turbulent viscoelastic flow with the orifice partly due to the Hadamard instability in viscoelastic-flow calculations [10]. In the present study, we executed DNS of a viscoelastic fluid in the same geometry with that of Makino *et al.* [9], using a composite flux-limiter (minmod) scheme to the convective term in the Giesekus-model constitutive equation and applying finer grids relative to existing similar works.

Major differences between the present study and published works on smooth channels are related to the streamwise variation of the flow state and the main areas where turbulence is produced. Therefore, the instantaneous vortex structures and the relevant momentum and heat transports within the strong shear layer just downstream of the orifice will be explored. Figure 8 presents an instantaneous snapshot of eddies, with emphasis on the orifice downstream, and surface distributions of temperature and wall heat flux, revealing high heat fluxes on the wall surface under the vortex motions. It is interesting to note that the wall heat flux also becomes intermittently high far downstream of the orifice, namely, at $x = 8-10$, where no apparent eddy is observed. Such heat-transfer enhancement leads to an increase of local Nusselt number compared with the Newtonian case, as can be seen in Fig. 9. Therefore, we draw a conclusion that this geometry gives rise to the dissimilarity between momentum and heat transports and the advantage of the heat transfer compared with the smooth channel. However, the present bulk Reynolds number ($Re_m \sim 1200$) was considerably lower than those corresponding conditions under which drag reduction in practical flow systems is observed with dilute additive solutions. It is necessary to further calculate viscoelastic flows at higher Reynolds numbers and with a wide range of rheological properties.

References

- [1] W. Bos, L. Liechtenstein, and K. Schneider, "Directional and scale-dependent statistics of quasi-static magnetohydrodynamic turbulence," *Phys. Rev. E* 76, 046310, 2007.
- [2] N. Okamoto, K. Yoshimatsu, K. Schneider, and M. Farge, "Directional and scale-dependent statistics of quasi-static magnetohydrodynamic turbulence," *ESAIM: Proceedings* (accepted).
- [3] Kong, H., Choi, H., and Lee, J. S., "Direct numerical simulation of turbulent thermal boundary layers," *Phys. Fluids*, 12, 2666, 2000.
- [4] Lund, T. S., Wu, X., and Squires, K. D., "Generation of turbulent inflow data for spatially-developing boundary layer simulations," *J. Comput. Phys.*, 140 (2), 1998, 233-258.
- [5] F. Hamba, "A Hybrid RANS/LES Simulation of Turbulent Channel Flow," *Theoret. Comput. Fluid Dynamics*, 16, 387-403, 2003.
- [6] H. Hiraoka and M. Ohashi, "A k- ϵ turbulence closure model for plant canopy flows," *Proc. of the 4th Int. Symp. on Comp. Wind Eng.*, 693-696, 2006.
- [7] A. Gyr and H. W. Bewersdorff, *Drag reduction of turbulent flows by additives*, Kluwer Academic Publisher, Dordrecht, Netherlands, 1995.
- [8] P. J. Oliveira, "Asymmetric flows of viscoelastic fluids in symmetric planar expansion geometries," *J. Non-Newtonian Fluid Mech.*, 114, 33-63, 2003.
- [9] S. Makino, K. Iwamoto, and H. Kawamura, "Turbulent structures and statistics in turbulent channel flow with two-dimensional slits," *Int. J. Heat & Fluid Flow*, 29, 602-611, 2008.
- [10] D. D. Joseph, *Fluid dynamics of viscoelastic liquids*, Springer-Verlag, New York., 1990.

乱流の世界最大規模直接数値計算とモデリングによる応用計算

プロジェクト責任者

金田 行雄 名古屋大学 大学院工学研究科

著者

金田 行雄 名古屋大学 大学院工学研究科

石原 卓 名古屋大学 大学院工学研究科

岩本 薫 東京農工大学 工学府

田村 哲郎 東京工業大学 大学院総合理工学研究科

川口 靖夫 東京理科大学 理工学部

塚原 隆裕 東京理科大学 理工学部

地球シミュレータ (ES2) を用いて、乱流の規範的 (カノニカル) な問題の大規模直接数値計算 (DNS) を実施した。具体的には (i) 世界最大レイノルズ数の平行平板間乱流 (ii) 磁場中の準定常 MHD 乱流、(iii) 正弦波状壁面上の乱流境界層の DNS である。これらの DNS は各々、(1) 高レイノルズ数壁乱流の対数領域における局所非等方性、(2) 磁場中の準定常 MHD 乱流における非等方性と間欠性、(3) 正弦波状壁面の波長が乱流等計量に与える影響、について研究するための貴重なデータを提供するものである。データ解析により、(1) 局所的な非等方性が壁から離れるに従って小さくなること、(2) 磁場が MHD 乱流場中の間欠性を強める働きがあること、(3) 正弦波の波長が小さくなるに従い圧力抵抗が増加することを見いだした。

我々はまた、これまでに得られた乱流統計の基礎的な知見に基づき、環境や工業的な応用問題として、以下の大規模数値計算を実施した。具体的には、(i) 適切かつ有効に粗面の条件を与えることが可能な LES と RANS のハイブリッドモデルを用いた計算により、一様な植生上で発達する乱流境界層の非定常解析を行った。また、(ii) 直方体型のオリフィスのあるチャンネル中の非ニュートン流体の乱流の DNS により、抵抗低減に伴う熱伝達率特性の評価に成功した。

キーワード: 大規模直接数値計算, 平行二平板間乱流, MHD 乱流, 乱流境界層, 粗面, LES, 都市型大気乱流境界層, 界面活性剤, 抵抗低減